Fluid Path Detection Model for Lab on a Chip Images Using Deep Learning-Based Segmentation Approach

Mahmood Khalghollah[1,3], Esmaeil Shakeri [1], Azam Zare[2], Behrouz H. Far[1], Amir Sanati-Nezhad[3]

[1] Department of Electrical and Software Engineering, Schulich School of Engineering, University of Calgary, Canada

[2] Department of Mechanical and Manufacturing Engineering, Schulich School of Engineering, University of Calgary, Canada

[3] Department of Biomedical Engineering, Schulich School of Engineering University of Calgary, Canada

{mahmood.khalghollah, esmaeil.shakerihosse, azam.zare, far, amir.sanatinezhad}@ucalgary.ca

Abstract

This paper explores the potential of Lab on a Chip (LOC) technologies in transforming diagnostic, biotechnology, and chemical/mechanical analysis fields. The proposed solution integrates advanced image processing into an automated tool, providing a robust and efficient method for precise data extraction from microfluidic chip images. In this study, we identify the fluid path in each frame, thereby improving the platform for tracking valuable fluid parameters over time, such as the viscosity of biofluids. Different patterns of LOC were developed then captured and related masks were established to create the 150 images dataset. Using the DeepLabv3+ deep learning model on the dataset, this study achieves remarkable validation accuracy of 98.95% and a low loss value of 0.012 for chip analysis path segmentation. The successful integration of DeepLabv3+ and meticulous preprocessing enhances understanding of fluid behavior within microfluidic chips, paving the way for advancements in chip design, diagnostics, and fluid feature-based analyses.

Introduction and Related Works

Lab on a Chip technologies have gained substantial attention for their potential to miniaturized and revolutionize diagnostic, bio-technology, and chemical and mechanical analysis. (Pattanayak et al., 2021) The development of passively driven microfluidic labs on chips has been increasing, with a focus on rapid, compact, portable, and easy-to-use devices. (Narayanamurthy et al., 2020) (Salahandish, Haghayegh, et al., 2022) The increasing demand for developing lab-on-a-chip (LOC) devices necessitates the improvement of the designing process to address the evolving needs and challenges in the field. (Salahandish, Jalali, et al., 2022) As innovations in designing, prototyping, and producing microfluidic chips continue to emerge, developers and manufacturers are finding solutions to common challenges in LOC device design and production to reduce the development time and expensive resources. However, the process of designing and debugging passively driven microfluidics and LOC is challenging and may take months or years while consuming valuable resources.

In the process of developing a new chip for specific purposes, we need to keep track of all the previous chip versions, study the effect of adding a new component and repeat all the experiments to exam the reliability of the functionality. For example, in the design process of a self-powered microfluidic based electrochemical biosensing platform for point-of-care quantification of proteins (Haghayegh et al., 2022) six main design were developed and investigated to present the final functional design, or eleven main design in developing an autonomous point-of-care testing (Salahandish, Hassani, et al., 2022) using conventional tools took a significant resources. Currently, the fluid interface position proceed in time as a key factor in the passively automated microfluidic chip are extracted manually by user using Fiji an opensource platform for image analysis. (Schindelin et al., 2012) However, analyzing and extracting fluid paths from the recorded videos, considering only a limited number of frames, may take weeks or even months for an expert user. This prolonged process can delay the design procedure and consume significant resources and energy.

Deep learning (DL) demonstrates a well-performed approach in machine learning where data is processed through layers of non-linear transformations in a hierarchical fashion, enabling the model to learn and extract features at various levels of extraction. (Lecun et al., 2015) (Shakeri, Mohammed, et al., 2023) Streamlining the segmentation task LOC processes can contribute to a prompter

and more effective outcome to enhance one of the buttle neck of microfluidic chip development process. Thus, introducing a platform to analyze the recorded videos of the experiments saves significant time and resources. DL models, such as convolutional neural networks (CNN) (Sengupta et al., 2020), can enhance ongoing research in the practical segmentation of chips by automatically modeling different outcomes and facilitating the analysis of chip paths detection. (Ganin & Lempitsky, 2014) Transfer Learning (TL) provides an alternative approach to address the constraints of DL models, tackling challenges like hyperparameter tuning complexity, preventing overfitting, and enhancing their generalizability. (Zhuang et al., 2021) (Shakeri et al., 2022)

Building upon this understanding, the following methodology section outlines our approach to image segmentation. Leveraging insights from the original need and addressing identified gaps, our proposed methodology employs advanced techniques to achieve high accuracy while minimizing computational resources. Next section provides an overview of the methods employed in our study, setting the stage for a detailed examination of our experimental design and results.

Methodology

For this work, we employed randomly selected frames from experiment-derived videos. Then, we generated masks for 150 images, facilitating the training of a DL model specialized in semantic segmentations. A comprehensive analysis of the model was conducted to determine the effectiveness of approach for identifying fluid paths within video frames. Through the extraction of predicted paths for all frames and the subtraction of sequential frames, we discerned the progression of fluid at distinct time intervals.

Data Generation

In order to develop this predictive model, we used our previously designed, fabricated and tested different network of patterns in microfluidic chips. Each complex pattern and network of microfluidic channels could be made with other elements. Thus, the patterns primarily consisted of limited fundamental elements, including straight or zigzag channels, split or merge joints, and inlets and ventilations as shown in Figure 1. The images from recorded videos were labeled to generate related masks based on the fluid path of that specific video frame in a chip in order to generate the dataset.[1]

[1] https://github.com/Mkh23/Fluid-Paths-Detection

Figure 1 Real images of fundamental elements filled by die water or blood, a) Straight Channel, b) Zigzag Channel, c) Splitting Joint, d) Merging Joint, e) Inlet, f) Ventilation.

Microfluidic Chip Design and Fabrication

The microscale elements and fluidic networks were fabricated by cutting the designed patterns on the pressure-sensitive adhesives (PSA) and Hydrophilic transparent polyethylene terephthalate (PET) using CO_2 Laser cutter. These chips would be one of the most affordable chips to make and easy to fabricate.

Experimental Setup and Data Gathering

The images were conducted from real experiments of microfluidic chip development process videos. Transparent sheets were chosen as the material for the chip, and a small quantity of dye was introduced into clear test biofluids such as water, tears, and sweat to facilitate their identification within the chip. Meanwhile, blood and serum retained their original coloration.

Data preparation and Labeling

In Python, a graphical user interface (GUI) was created using TKinter and OpenCV libraries to designate paths on images. This custom-built application assists users in generating masks for individual image frames. Various recording devices, including smartphones and DSLR cameras, were employed for video capture. Consequently, all images and masks were standardized to 512 x 512 pixels to enhance processing speed and ensure uniform input image dimensions. Interpolation followed by a stringent threshold was applied to resize the masks, preventing any loss during the resizing process.

As the data source for monitoring outcomes in this study is based on image processing, we applied a series of image preprocessing techniques before using the data into the training process. These techniques include image resizing, and data augmentation. **Image resizing**: An input image in chip is characterized by three parameters: W × H × C, where W denotes the width, H signifies the height, and C represents the number of channels in the image. (Rafi & Shubair, 2021) (Shakeri, Crump, et al., 2023) To ensure uniformity in the dimensions of our input data and align them with the data utilized in pre-trained models, we resized our input data to 512×512×3 for the DeepLabV3+ model. **Data augmentation**: To augment the training set size, enhance the performance and generalizability of our predictive models, and mitigate model overfitting con-

cerns, we employed the Album library in PyTorch for image augmentation. Specifically, we applied techniques such as image rotation, along with vertical and horizontal flipping, to simulate potential variations in chip path orientations. For the binary segmentation of chip path analysis, we rescaled the provided images by a factor of 1/255, effectively bringing the pixel values within the range of 0 to 1.

Segmentation models

This section explains information on the customized and optimized deep learning architectures developed to suit the unique characteristics of our dataset and the specific requirements of our study. In this work, for the segmentation of the chip dataset aimed at fluid path analysis, we applied advanced deep learning model, specifically opting for DeepLabV3+.(Chen et al., 2017)(Yurtkulu et al., 2019). The ResNet-50 or ResNet-101 network as the backbone model for feature extraction were investigated. The ResNet-50, a 50-layer deep neural network, provides a good balance between accuracy and computational cost. On the other hand, the ResNet-101, with its deeper architecture, delivers enhanced performance without a substantial increase in computational complexity. The DeepLabv3+ model leverages the features extracted by these backbone networks to enhance its semantic segmentation capabilities. (Wang et al., 2022)

In this research, we applied ReseNet-101 (He et al., 2016) an encoder known as a transfer learning model with numerous convolutional layers, a crucial factor that effectively reduces the number of parameters utilized in the learning process of the deconvolution network for semantic segmentation. (Sreelakshmi et al., 2023) The employment of the sigmoid (Nieradzik et al., 2021) activation function, known as the standard output activation in neural network segmentation tasks, was implemented in the deep learning models. A ratio of 0.1 was applied to split the chip dataset 140 images for training and 10 for validating images.

Configuration

We iterated through the entire training and evaluation process for the chip segmentation task, using batch size values set at 8. We generated plots depicting intersection over union (IoU) (Rezatofighi et al., 2019), and Dice similarity coefficient (DSC) (Andrews & Hamarneh, 2015) for the loss values across all epochs to verify that the model's performance was not influenced by overfitting. We employed PyTorch, recognized as a high-performance deep learning library (Paszke et al., 2019) trained and evaluated a dataset of 43 MB uploaded in GitHub, consisting of 150 filled microfluidic chip RGB images, using CPU 11th Gen Intel(R) Core (TM) i7-1185G7 @ 3.00GHz and 9 GB memory RAM for 6 hours of 60 training epochs. We utilized IoU and DSC values for training and validating the prediction models created in this study. Moreover, we experimented with various hyperparameter values to configure the predictive segmentation model. After testing different options, we found that utilizing the Adam optimizer (Kingma & Ba, 2014) and setting the learning rate to 0.0001 resulted in the optimal performance, and these settings were employed in our customized deep learning models. (Jepkoech et al., 2021) We used transfer learning Resent101 (He et al., 2016) as encoder model for training and validating the segmentation results of chip path segmentation. We implemented weightings as a technique to tackle the data imbalance problem present in our dataset. (Guo & Viktor, 2004) To further mitigate this challenge, we incorporated the ImageNet pre-trained model into our training process. This addition provided additional context, enhancing the learning speed and overall accuracy of our model. (Krizhevsky et al., 2012) In our experimentation, we initially set the number of training epochs to 60 based on empirical observations to achieve the highest accuracy in both the training and validation sets. However, we noticed that the performance plateaued after reaching certain epochs, particularly around the 55th epoch. Consequently, to conserve computational resources, we opted for fewer epochs in this study.

Results

To assess the performance of our proposed methodology, we conducted evaluation on a set of sample test images. We quantitatively evaluated the performance of DeepLabv3+ model using standard metrics such as Dice loss, IoU Score, F-Score and confusion matrix as shown in Figure 2. Our DeepLabv3+ model, trained with the Dice loss, showed great results, especially at the 60th epoch. For the training dataset, the Dice loss was impressively low at 0.012, and the IoU score and F-Score were high at 0.9904 and 0.9952, respectively. Similarly, on the validation dataset, the Dice loss was minimal at 0.013, with an IoU score of 0.9895 and an F-Score of 0.9947. These values indicate strong performance. We also used a confusion matrix to visually represent how well the model classified different classes. These findings confirm that our approach works well, demonstrating the DeepLabv3+ model's proficiency in semantic image segmentation tasks.

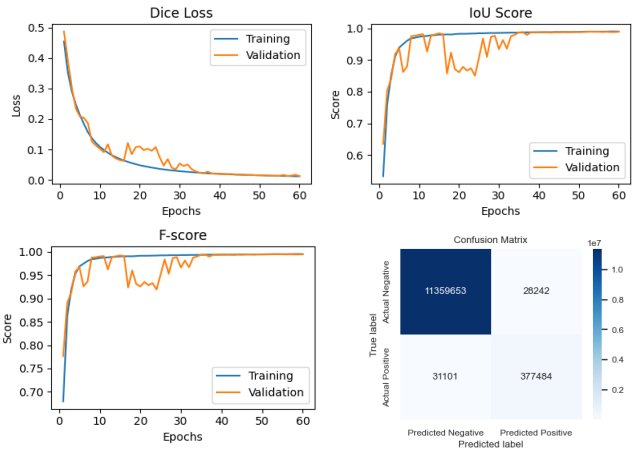

Figure 2 Performance evaluation of training the model in 60 epochs with Dice loss, IoU Score, F-Score and Confusion matrix.

The sample results presented in Figure 3 depict a middle frame for a split-merge-mixing chip, providing a visual representation of the model's segmentation performance. The figures include the Original Image, Ground Truth Mask, Predicted Mask, and Predicted Path Heatmap. Notably, this chip represents a scenario with intricate structures and complex paths, making it a challenging test case. The model's ability to accurately delineate and predict the paths within this mid-frame is a testament to its effectiveness in capturing nuanced details.

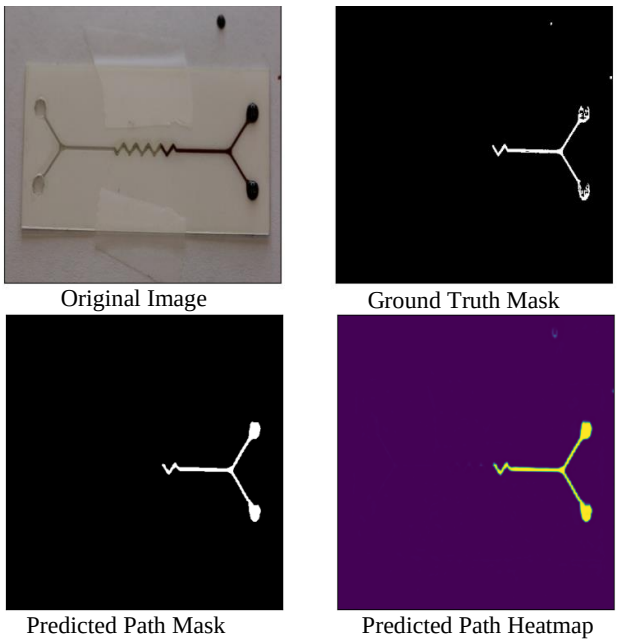

Figure 3 The Original Image depicting a mixing microfluidic chip during the filling process with a droplet of blood. The predicted mask and fluid paths are overlaid.

In Figure 4, we showcase the final frame for a merge-split-mixing chip, which is considered one of the most intricate configurations among the chips examined. The results reveal the model's remarkable capability to navigate and accurately predict the complex paths in the final frame of this chip. The fidelity between the Ground Truth Mask and the Predicted Mask underscores the model's proficiency in semantic image segmentation, particularly in scenarios involving intricate chip structures. These exemplary results affirm the effectiveness of the DeepLabv3+ model in handling the challenges posed by diverse chip configurations.
This model exhibits strong performance by attaining an impressive validation accuracy of 98.95%, efficiently capturing pertinent features within the sample test images while maintaining low CPU usage. Therefore, it holds the potential to generate predicted masks for successive frames in any experiment. This analysis can be performed in real-time during video capture in the laboratory, delivering accurate results simultaneously.

Limitations

Some limitations might infect the performance results of this study. We exclusively applied a single deep learning model for the segmentation of chip path analysis. Utilizing different models on the same dataset could potentially yield varied results for binary segmentation. Furthermore, we utilized a small dataset comprising 150 chip images to

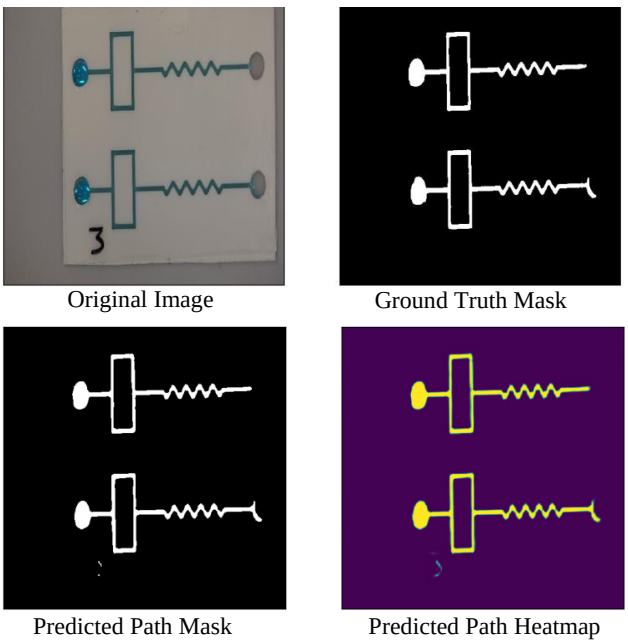

Figure 4 The Original Image captures the final frame of a video, showcasing a microfluidic chip filled with a droplet of saliva, depicting the complete path traversed by the fluid. The predicted mask and fluid paths are depicted alongside.

train and evaluate our deep-learning models, which could potentially restrict the generalizability of our findings. To overcome this limitation, we employed data augmentation in PyTorch to expand the dataset's size. This approach aimed to enhance the accuracy of our models and mitigate issues associated with the dataset's small size.

Conclusion

In this paper, we introduce a deep learning model, DeepLabv3+, designed to predict masks and fluid paths within microchannel networks on a chip. Leveraging fluid position data, our model accurately delineates fluid paths, offering valuable insights into fluid dynamics within microfluidic systems. The extracted data is then subjected to comprehensive analysis, enabling comparison of video frames to track fluid progression through the network. We conducted experiments using various biofluids, including water, sweat, tear, saliva, serum, and blood, yielding promising results that underscore the model's high accuracy in identifying fluid paths. Notably, our model significantly reduces the time required for professional microfluidic chip developers to annotate fluid paths across all frames of an experimental video, offering a streamlined and efficient approach for microfluidic chip analysis, development and debugging.

Future Work

Expanding the application scope of our fluid path detection system opens up numerous possibilities for advancing research and addressing practical challenges in various fields. One avenue for future exploration involves delving deeper into the analysis of biofluid behaviors beyond simple fluid path detection. By leveraging the capabilities of the DeepLabv3+ model and integrating additional analytical tools, we can extend our investigations to encompass a wide range of applications. **Viscosity Analysis**: Further research can focus on quantifying and analyzing the viscosity of biofluids, such as blood, using the proposed methodology. By correlating changes in fluid behavior captured by the model with known viscosity profiles, we can develop non-invasive techniques for real-time viscosity estimation, with potential applications in medical diagnostics and drug delivery systems. **Real-Time Monitoring and control**: Integrating the proposed system with real-time monitoring and control mechanisms facilitates dynamic adjustments and interventions based on observed fluid behaviors. By continuously analyzing video streams and subtracting predicted masks from consecutive frames, deviations in fluid flow patterns can be detected and addressed in real-time, enabling adaptive control strategies for optimizing process efficiency and reliability. **Multi-Modal Imaging Fusion**: Combining the outputs of the DeepLabv3+ model with other imaging modalities, such as chemiluminescence methods enhances the richness of information of reaction and sensing captured. By fusing data from multiple sources, we can obtain a more comprehensive understanding of fluid dynamics, spatial distribution of biochemical species, and structural characteristics within microfluidic networks.

Acknowledgement

The authors acknowledge the Canada Research Chair, NSERC CREATE Wearable Technology Research and Collaboration (We-TRAC) Training Program (Project No. CREATE/511166-2018), University of Calgary.

References

Andrews, S., & Hamarneh, G. (2015). Multi-region probabilistic dice similarity coefficient using the Aitchison distance and bipartite graph matching. *ArXiv Preprint ArXiv:1509.07244*.

Chen, L.-C., Papandreou, G., Schroff, F., & Adam, H. (2017). Rethinking atrous convolution for semantic image segmentation. *ArXiv Preprint ArXiv:1706.05587*.

Ganin, Y., & Lempitsky, V. (2014). -fields: neural network nearest neighbor fields for image transforms. *Asian Conference on Computer Vision*, 536–551.

Guo, H., & Viktor, H. L. (2004). Learning from imbalanced data sets with boosting and data generation: the databoost-im approach. *ACM Sigkdd Explorations Newsletter*, *6*(1), 30–39.

Haghayegh, F., Salahandish, R., Zare, A., Khalghollah, M., & Sanati-Nezhad, A. (2022). Immuno-biosensor on a chip: a self-powered microfluidic-based electrochemical biosensing platform for point-of-care quantification of proteins. *Lab on a Chip*, *22*(1), 108–120. https://doi.org/10.1039/d1lc00879j

He, K., Zhang, X., Ren, S., & Sun, J. (2016). Deep residual learning for image recognition. *Proceedings of the IEEE Conference on Computer Vision and Pattern Recognition*, 770–778.

Jepkoech, J., Mugo, D. M., Kenduiywo, B. K., & Too, E. C. (2021). *The effect of adaptive learning rate on the accuracy of neural networks*.

Kingma, D. P., & Ba, J. (2014). Adam: A method for stochastic optimization. *ArXiv Preprint ArXiv:1412.6980*.

Krizhevsky, A., Sutskever, I., & Hinton, G. E. (2012). Imagenet classification with deep convolutional neural networks. *Advances in Neural Information Processing Systems*, *25*.

Lecun, Y., Bengio, Y., & Hinton, G. (2015). Deep learning.

Nature, *521*(7553), 436–444. https://doi.org/10.1038/nature14539

Narayanamurthy, V., Jeroish, Z. E., Bhuvaneshwari, K. S., Bayat, P., Premkumar, R., Samsuri, F., & Yusoff, M. M. (2020). Advances in passively driven microfluidics and lab-on-chip devices: A comprehensive literature review and patent analysis. *RSC Advances*, *10*(20), 11652–11680. https://doi.org/10.1039/d0ra00263a

Nieradzik, L., Scheuermann, G., Saur, D., & Gillmann, C. (2021). Effect of the output activation function on the probabilities and errors in medical image segmentation. *ArXiv Preprint ArXiv:2109.00903*.

Paszke, A., Gross, S., Massa, F., Lerer, A., Bradbury, J., Chanan, G., Killeen, T., Lin, Z., Gimelshein, N., & Antiga, L. (2019). Pytorch: An imperative style, high-performance deep learning library. *Advances in Neural Information Processing Systems*, *32*.

Pattanayak, P., Singh, S. K., Gulati, M., Vishwas, S., Kapoor, B., Chellappan, D. K., Anand, K., Gupta, G., Jha, N. K., Gupta, P. K., Prasher, P., Dua, K., Dureja, H., Kumar, D., & Kumar, V. (2021). Microfluidic chips: recent advances, critical strategies in design, applications and future perspectives. *Microfluidics and Nanofluidics*, *25*(12), 1–28. https://doi.org/10.1007/s10404-021-02502-2

Rafi, T. H., & Shubair, R. M. (2021). A scaled-2d cnn for skin cancer diagnosis. *2021 IEEE Conference on Computational Intelligence in Bioinformatics and Computational Biology (CIBCB)*, 1–6.

Rezatofighi, H., Tsoi, N., Gwak, J., Sadeghian, A., Reid, I., & Savarese, S. (2019). Generalized intersection over union: A metric and a loss for bounding box regression. *Proceedings of the IEEE/CVF Conference on Computer Vision and Pattern Recognition*, 658–666.

Salahandish, R., Haghayegh, F., Ayala-Charca, G., Hyun, J. E., Khalghollah, M., Zare, A., Far, B., Berenger, B. M., Niu, Y. D., Ghafar-Zadeh, E., & Sanati-Nezhad, A. (2022). Bi-ECDAQ: An electrochemical dual-immuno-biosensor accompanied by a customized bi-potentiostat for clinical detection of SARS-CoV-2 Nucleocapsid proteins. *Biosensors and Bioelectronics*, *203*(January), 114018. https://doi.org/10.1016/j.bios.2022.114018

Salahandish, R., Hassani, M., Zare, A., Haghayegh, F., & Sanati-Nezhad, A. (2022). Autonomous electrochemical biosensing of glial fibrillary acidic protein for point-of-care detection of central nervous system injuries. *Lab on a Chip*, *22*(8), 1542–1555. https://doi.org/10.1039/d2lc00025c

Salahandish, R., Jalali, P., Tabrizi, H. O., Hyun, J. E., Haghayegh, F., Khalghollah, M., Zare, A., Berenger, B. M., Niu, Y. D., & Ghafar-Zadeh, E. (2022). A compact, low-cost, and binary sensing (BiSense) platform for noise-free and self-validated impedimetric detection of COVID-19 infected patients. *Biosensors and Bioelectronics*, *213*, 114459.

Schindelin, J., Arganda-Carreras, I., Frise, E., Kaynig, V., Longair, M., Pietzsch, T., Preibisch, S., Rueden, C., Saalfeld, S., Schmid, B., Tinevez, J. Y., White, D. J., Hartenstein, V., Eliceiri, K., Tomancak, P., & Cardona, A. (2012). Fiji: An open-source platform for biological-image analysis. *Nature Methods*, *9*(7), 676–682. https://doi.org/10.1038/nmeth.2019

Sengupta, S., Singh, A., Leopold, H. A., Gulati, T., & Lakshminarayanan, V. (2020). Ophthalmic diagnosis using deep learning with fundus images–A critical review. *Artificial Intelligence in Medicine*, *102*, 101758.

Shakeri, E., Crump, T., Weis, E., Mohammed, E., Souza, R., & Far, B. (2023). Explaining Eye Diseases Detected by Machine Learning Using SHAP: A Case Study of Diabetic Retinopathy and Choroidal Nevus. *SN Computer Science*, *4*(5), 433.

Shakeri, E., Crump, T., Weis, E., Souza, R., & Far, B. (2022). Using SHAP Analysis to Detect Areas Contributing to Diabetic Retinopathy Detection. *Proceedings - 2022 IEEE 23rd International Conference on Information Reuse and Integration for Data Science, IRI 2022*, 166–171. https://doi.org/10.1109/IRI54793.2022.00046

Shakeri, E., Mohammed, E., Crump, T., Weis, E., Shields, C. L., Ferenczy, S. R., & Far, B. (2023). Deep Learning-Based Detection and Classification of Uveal Melanoma Using Convolutional Neural Networks and SHAP Analysis. *2023 IEEE 24th International Conference on Information Reuse and Integration for Data Science (IRI)*, 215–220. https://doi.org/10.1109/IRI58017.2023.00044

Sreelakshmi, S., Malu, G., Sherly, E., & Mathew, R. (2023). M-Net: An encoder-decoder architecture for medical image analysis using ensemble learning. *Results in Engineering*, *17*, 100927.

Wang, Y., Wang, C., Wu, H., & Chen, P. (2022). An improved Deeplabv3+ semantic segmentation algorithm with multiple loss constraints. *PLoS ONE*, *17*(1 January), 1–14. https://doi.org/10.1371/journal.pone.0261582

Yurtkulu, S. C., Sahin, Y. H., & Bili, B. (2019). *Geni ¸ sletilmi ¸ s DeepLabv3 Mimarisi ile Anlamsal Bölütleme Semantic Segmentation with Extended DeepLabv3 Architecture*. 10–13.

Zhuang, F., Qi, Z., Duan, K., Xi, D., Zhu, Y., Zhu, H., Xiong, H., & He, Q. (2021). A Comprehensive Survey on Transfer Learning. *Proceedings of the IEEE*, *109*(1), 43–76. https://doi.org/10.1109/JPROC.2020.3004555